





Review

Heterometal Grafted Metalla-ynes and Poly(metalla-ynes): A Review on Structure–Property Relationships and Applications

Rayya A. Al-Balushi ^{1,*}, Ashanul Haque ^{2,*}, Idris J. Al-Busaidi ³, Houda Al-Sharji ⁴
and Muhammad S. Khan ^{4,*}

¹ Department of Basic Sciences, College of Applied and Health Sciences, A'Sharqiyah University, P.O. Box 42, Ibra 400, Oman

² Department of Chemistry, College of Science, University of Hail, Ha'il 81451, Saudi Arabia

³ The Directorate General of Private Schools, Ministry of Education, P.O. Box 3, Muscat 100, Oman; idris.albusaidi.oman@gmail.com

⁴ Department of Chemistry, Sultan Qaboos University, P.O. Box 36, Al-Khod 123, Oman; houda.sultan91@gmail.com

* Correspondence: rayya.albalushi@asu.edu.om (R.A.A.-B.); a.haque@uoh.edu.sa (A.H.); msk@squ.edu.om (M.S.K.)

Abstract: Metalla-ynes and poly(metalla-ynes) have emerged as unique molecular scaffolds with fascinating structural features and intriguing photo-luminescence (PL) properties. Their *rigid-rod* conducting backbone with tunable photo-physical properties has generated immense research interests for the design and development of application-oriented functional materials. Introducing a second *d*- or *f*-block metal fragment in the main-chain or side-chain of a metalla-yne and poly(metalla-yne) was found to further modulate the underlying features/properties. This review focuses on the photo-physical properties and opto-electronic (O-E) applications of heterometal grafted metalla-ynes and poly(metalla-ynes).

Keywords: metalla-ynes; poly(metalla-ynes); polymers; opto-electronic; photo-physical



Citation: Al-Balushi, R.A.; Haque, A.; Al-Busaidi, I.J.; Al-Sharji, H.; Khan, M.S. Heterometal Grafted Metalla-ynes and Poly(metalla-ynes): A Review on Structure–Property Relationships and Applications. *Polymers* **2021**, *13*, 3654. <https://doi.org/10.3390/polym13213654>

Academic Editor: Young-Gi Kim

Received: 30 August 2021

Accepted: 20 October 2021

Published: 23 October 2021

Publisher's Note: MDPI stays neutral with regard to jurisdictional claims in published maps and institutional affiliations.



Copyright: © 2021 by the authors. Licensee MDPI, Basel, Switzerland. This article is an open access article distributed under the terms and conditions of the Creative Commons Attribution (CC BY) license (<https://creativecommons.org/licenses/by/4.0/>).

1. Introduction

Metalla-ynes and poly(metalla-ynes) are *rigid-rod* type molecular systems in which one or more transition metal ions are connected to the alkynyl unit via σ -linkage [1,2]. Owing to their excellent photo-luminescence (PL) properties, structural features and diverse applications, this class of materials has received significant attention in the last two decades. In this class of materials, the electronic structure and properties are a function of the overall chemical composition of the material, i.e., type of organic spacers, no. of alkynyl units, metal fragments, and auxiliary ligands attached to the metals [1,3–5]. For instance, the introduction of a heavy transition metal ion into the backbone of organic poly-yne core induces spin–orbit coupling (SOC) and facilitates intersystem-crossing (ISC) leading to efficient photo-luminescence quantum yield (PLQY) [6–9]. Similarly, when an electron-rich (donor, D) and an electron-deficient (acceptor, A) organic spacers are introduced, it creates a strong intramolecular D-A interaction leading to absorption and emission extending from the visible to near-infrared (NIR) region of the spectrum [10–14]. The impact of topology (point of attachment) on the photo-physical properties (such as isomerization) was also established [15,16]. Several functional materials have been developed with potential application in molecular electronics, photo-voltaic, organic light-emitting diodes (OLEDs), bioimaging, catalysis, etc. [3,17,18].

Among the various strategies adopted by researchers, the introduction of a second metal ion into the main-chain or as side-chain of the metalla-ynes and poly(metalla-ynes) is a judicious way to fine-tune their PL features. Several complexes in which *d*-block and

f-block metal fragments are connected through conjugated [19] and non-conjugated [20] linkers were reported in the literature. It is to be noted that the high conductivity, preservation of conjugation through the metal fragment, high triplet yield, etc. make “*d*” fragment a matter of choice for the metalla-yne and poly(metalla-yne) [21]. The heterometallic complexes bearing conjugated metalla-yne fragments often display modulated properties due to the synergistic effect of the two different metal ions [2,3,22–25]. For example, it is reported that combining two transition metal (*d-d*) fragments in an alkynyl complex affects the energy of the frontier molecular orbitals, emission lifetime [26], and, to some extent, solid-state packing [27]. Similarly, it was demonstrated that in mixed metal alkynyl complexes, the metalla-yne core sensitizes NIR lanthanide luminescence [28] and improves decay lifetime (from μs to ms) [29] via *d* → *f* energy transfer pathways. Inspired by this heterometallic cooperativity, numerous complexes were reported with *d-d* and *d-f* combinations [20,29–37]. We present herein a review of the photo-physical properties and O-E applications of heterometal grafted metalla-yne and poly(metalla-yne). In this paper, we considered only those examples in which *d-d* and *d-f* fragments are separated by one or more alkynyl units (Figure 1). Both, the main-chain, and side-chain metalla-yne and poly(metalla-yne) were considered to get a clear picture.

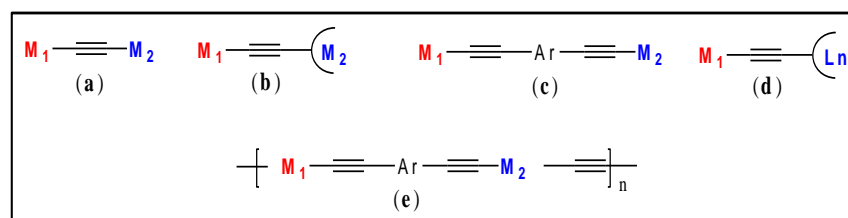


Figure 1. General chemical structure of some of the *d-d* and *d-f* fragments containing heterometallic complexes. M_1 and M_2 = transition metal ions (a), Ln = a lanthanide core (b), Ar = conjugated carbocyclic/heterocyclic spacers and (c) semi-circle = bi- (d) or polydentate donor ligands (e).

2. Impact on Properties

2.1. Main-Chain Systems

Transition metal complexes display a multitude of colorful optical (absorption/emission) and interesting magnetic properties due to the presence of metal ions in different oxidation states [38]. Moreover, multi-dimensional applications of transition metal complexes are well established [39]. It is well demonstrated that when one or more transition metal ions (decorated with suitable auxiliary ligands) are embedded in an organic framework via σ -linkage, new conducting materials are realized with limitless features and properties. Such materials, commonly known as metalla-yne or poly(metalla-yne), were studied and reviewed by several groups [40]. Both homo- and heterometallic σ -acetylide metal complexes with one or more types of transition metal ions are known in the literature, with a majority on homometallic systems [1,2]. The combination of two transition metals provides an effective way to realize new materials with unique structural features and improved properties such as high solubility and transparency [41]. Although heterometallic poly-yne containing Ni/Pt and Pd/Pt have been known for a long time [42,43], focus on using other metals has been sparse, possibly due to the challenging synthesis of suitable monomers and/or polymers. In this sub-section, we exemplify the structure and properties of heterometallic molecular systems while clusters [44] are beyond the scope of this paper. Attempts were made to include recent references that have not been covered before [25].

Dixneuf and co-workers [45] reported the first one dimensional Ru(II)/Pd(II) mixed metalla-yne as a yellow oligomer in good yield (84%) and moderate chain length ($M_w = 14,800$, $M_n = 7800$). Basic structural characterization showed the formation of mixed metalla-yne but no photo-physical properties were reported. Wong and co-workers [46] reported the very first example of *soluble* rigid-rod heteronuclear Pt(II)/Hg(II) poly(metalla-yne) (**P1**, Figure 2) and their corresponding model complexes. The reported white polymer exhibits

excellent thermal stability ($T_d = 366 \pm 5$ °C), and polydispersity ($M_w = 29,790$, $M_n = 15,704$, Table 1). The fluorescence quantum yield of the heterobimetallic polymer ($\Phi_f = 0.52$ in DCM, Table 1) was found to be lower than the homometallic *trans* polymers ($\Phi_f = 2.53$ for Hg(II) and 0.62 for Pt(II) in DCM) but higher than the *cis* counterpart ($\Phi_f = 0.1$ in DCM). Similarly, the heterometallic Pt(II)/Hg(II) complex showed a weak triplet emission at room temperature (RT) and a slightly stronger optical power limiting (OPL) performance than the homo-nuclear Hg(II) complexes. The transparency window of the poly-ynes in the visible regime coupled with their OPL performance was achieved by interrupting π -conjugation via copolymerization with Hg and tuning the Pt geometry (*cis* and *trans*).

A comparative study on homo- and heterometallic poly-ynes (**P1–P3**, Figure 2) indicated that Hg(II) and Pt(II) containing poly-ynes are better candidates for OPL than the corresponding Pd(II) poly-ynes as the former display absorption maxima below 400 nm [47]. It was shown that the heterometallic complex **P1** shows better transparency (maximum absorption wavelength (λ_{max}) = 386 nm, Table 1) than that of homometallic Pt(II) complexes (Figure 3). Theoretical calculations suggested that in heterometallic complexes, the contribution of d_π orbitals to the highest occupied molecular orbital (HOMO) was more from Pd/Pt than the Hg. Conversely, the contribution of p_π orbitals to the lowest unoccupied molecular orbital (LUMO) was more from the Hg fragment, in line with the earlier studies [46].

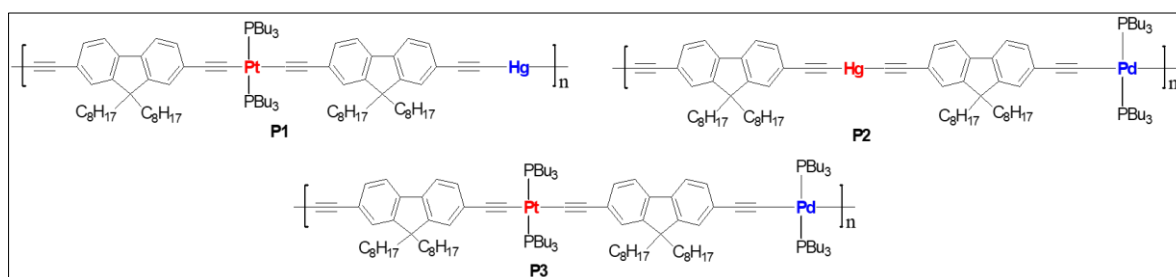


Figure 2. Heterometallic poly(metalla-ynes) **P1–P3**.

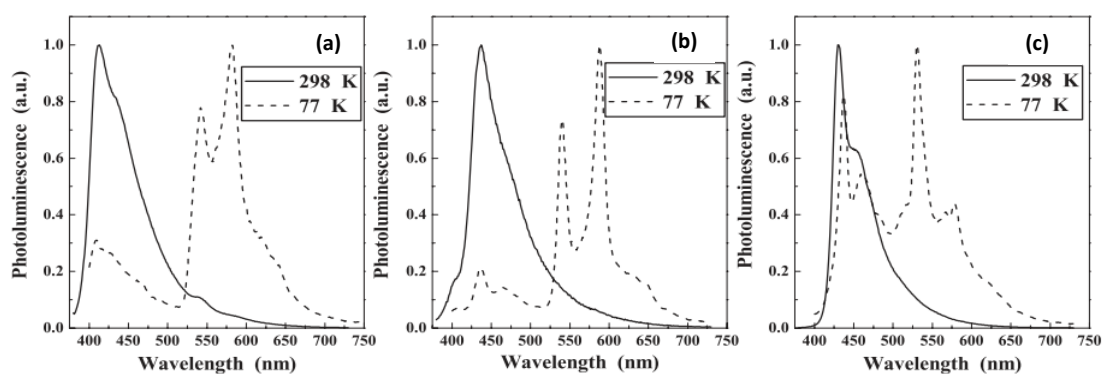


Figure 3. Photoluminescence (PL) spectra at 298 K and 77 K in CH_2Cl_2 for (a) **P1**, (b) **P3**, and (c) **P2**. Reproduced with permission from ref. [47].

In 2005, Vicente et al. [48] reported the very first examples of Pt(II)/Au(I) heterometallic anionic poly(metalla-ynes) **P4** and **P5** (Figure 4). The polymers, obtained by reacting Pt(II) *bis*- or *tetra* acetylides with $\text{PPN}[\text{Au}(\text{acac})_2]$ (PPN = *bis*(triphenylphosphine)iminium cation, acac = acetylacetonate) were poorly characterized due to the extremely low solubility. The only polymer **P5** (R = Bu) was soluble and could be characterized by nuclear magnetic resonance (^1H , ^{13}C , and ^{31}P NMR) and gel permeation chromatography (GPC) techniques, which showed comparatively good chain length of the polymers (up to 667 units).

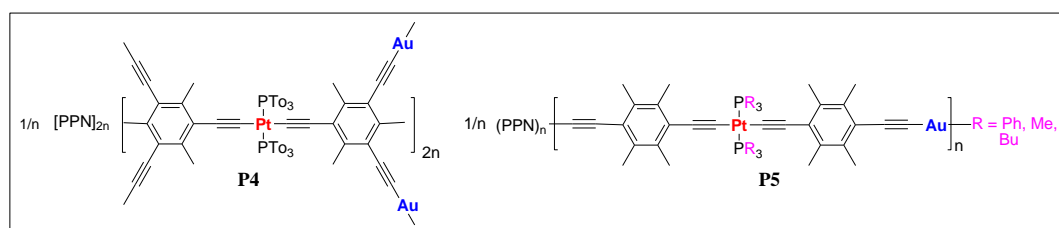


Figure 4. Pt(II)/Au(I) heterometallic anionic poly(metalla-ynes) **P4** and **P5**. (PPN = bis(triphenylphosphine)iminium cation).

Table 1. Photoluminescence (PL) data of some selected heterometallic poly(metalla-ynes) **P1–P3** and **P6–P11**.

Code	Metals	Molecular Weight ($\times 10^4$)		λ_{abs} (nm)	λ_{ems} (nm)	Lifetime of S_1 (τ^a , ns)	Lifetime of T_1 (τ^b , μ s)	Φ (%)	E_g (eV)	Ref.
		M_w	M_n							
P1	Pt/Hg	2.9	1.5	386	409 ^a , 542 ^b , 582 ^b	1.23	194.38, 202.84	0.52	3.01	[46]
P2	Pd/Hg	0.45	0.40	411	430 ^a , 544 ^b , 578 ^b	0.92	12.19, 22.71	12.60	2.85	[47]
P3	Pt/Pd	2.5	1.3	415	437 ^a , 540 ^b , 588 ^b	0.89	193.7, 188.2	0.60	2.83	[47]
P6	Pt/Au	-	2.4	270, 276, 305, 319, 345, 362, 387	417 ^a , 438 ^a , 450 ^a , 539 ^a , 548 ^b , 587 ^b , 625 ^b , 642 ^b	0.71	181.63	1.03	2.98	[22]
P7	Pt/Au	-	2.7	264, 276, 316sh, 377	504 ^a , 504 ^b , 545 ^b , 563 ^b	10370	130.80	0.62	3.00	[22]
P8	Pt/Au	-	2.9	253, 262, 276sh, 317, 335	405 ^a , 425 ^a , 455 ^a , 495 ^a , 534 ^a , 456 ^b , 492 ^b , 507 ^b , 527 ^b	0.99	44.31	0.27	3.19	[22]
P9	Pt/Au	-	2.1	275, 305, 319, 344, 361, 384	412 ^a , 432 ^a , 449sh ^a , 542 ^a , 584 ^a , 548 ^b , 586 ^b , 619 ^b	0.63	137.84	1.66	3.00	[22]
P10	Pt/Au	-	2.4	268, 275, 314sh, 373	504 ^a , 503 ^b , 529 ^b , 603 ^b	6460	165.23	1.69	3.01	[22]
P11	Pt/Au	-	3.1	253, 261, 316, 334	402 ^a , 421 ^a , 438 ^a , 455 ^a , 503 ^a , 457 ^b , 493 ^b , 507 ^b	0.72	40.14	0.30	3.12	[22]

M_w : average weight molecular weight, M_n : number weight molecular weight, λ_{abs} : absorption wavelength peaks, λ_{ems} : emission wavelength peaks, sh: shoulder, a: measured at 298 K, b: measured at 77 K, Φ : quantum yield, E_g : energy gap.

Wong and co-workers [22] reported heterometallic Au(I)–Pt(II) poly(metalla-ynes) (**P6–P11**, Figure 5), in which the impact of merging two different metals can be clearly observed (Table 1). Compared to the homometallic systems, Au(I)–Pt(II) poly(metalla-ynes) showed blue-shifted absorption maxima and cut-off absorption wavelengths in solution slightly shifted with respect to monomeric Pt(II) complexes. Merging two different metallic cores also significantly improved the transparency of the resulting material, which was attributed to the weak metal-ligand interactions and conjugation interruption by auxiliary ligands.

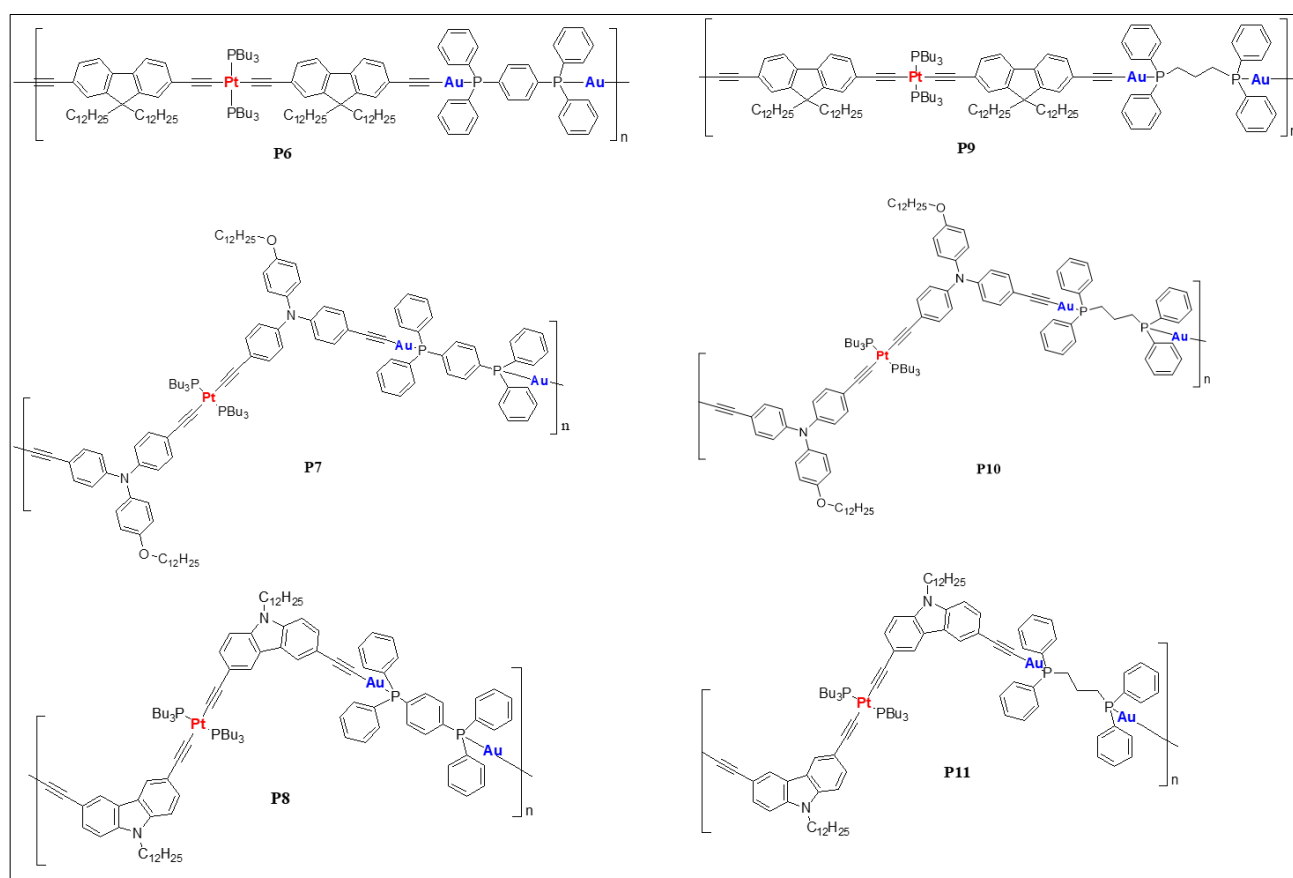


Figure 5. Heterometallic Au(I)–Pt(II) poly(metalla-yne)s (**P6–P11**) reported by Wong et al. [22].

2.2. Side-Chain Systems

2.2.1. *d-d* Metal-Containing Systems

Compared to the main chain heterometallic systems, dimers and polymers with second organometallic fragments attached via chelating ligand are more common in the literature. Several oligo- and poly(metalla-yne)s bearing heterometallic fragments were synthesized and studied in the past. In this section, we discuss some pertinent examples of both small and large molecular systems with two or more types of metal ions. As observed in the earlier examples, the inclusion of a second metal affects the PL properties. Among *d-d* combinations, the use of Ir(III) and Re(I) with Pt(II) metalla-yne)s is very common as the mixed-metal systems show improved photo-physical behavior [49]. It is well established that the photo-physical properties of a material are the function of the molecular structure of the main-chain and pendant ligands. Studies on heterometallic branched complexes indicated that the absorption and emission energies shift to the red upon the incorporation of the Pd(II) fragment moiety [50]. Compared to monometallic Re(I) complexes (maximum absorption wavelength (λ_{max}^{abs}) = 408–418 nm), trimetallic complexes **O1** (R = H or Me, Figure 6) exhibit low energy transition at λ_{max}^{abs} = 416–426 nm in solution (Table 2). Similarly, in tetrahydrofuran (THF) solution at RT, Re(I) complexes showed maximum emission wavelength (λ_{max}^{em}) at 625–636 nm (lifetime, τ_0 = < 0.1 μ s), while Pd(II)/Re(I) complexes emitted at λ_{max}^{em} = 628–639 nm (τ_0 = < 0.1 μ s, Table 2). Heterometallic complex **O2** (Figure 6) bearing Pd(II)/Ru(II) core exhibits highly red shifted absorption band (Table 2) compared to monometallic Ru(II)-counterpart [51].

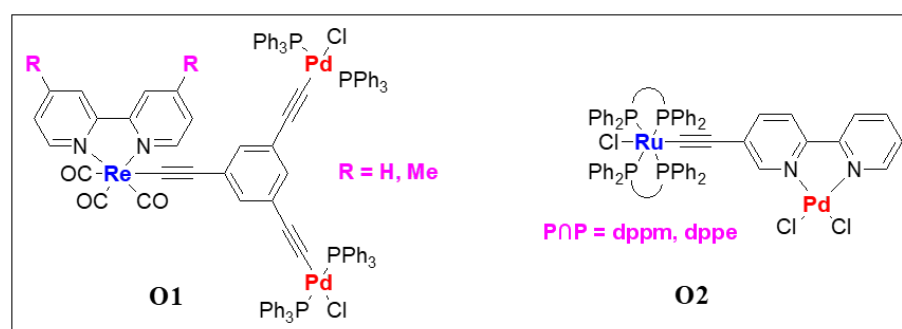


Figure 6. Re(I)/Pd(II) hetero-trimetallic (**O1**) and Ru(II)/Pd(II) heterometallic (**O2**) complexes.

Piazza and coworkers [52] assessed the photo-physical and magnetic properties of Ru(II)/Cu(I) and Ru(II)/Mn(I) couples **O3** and **O4** (Figure 7). Interestingly, a long-distance magnetic coupling between the terminal Cu(II) units through Ru(II) fragment was noted. Moreover, heterometallic systems displayed low energy bands in the visible region (Table 2). Cu(II) complexes exhibit higher thermal stability compared to Mn(I) complexes.

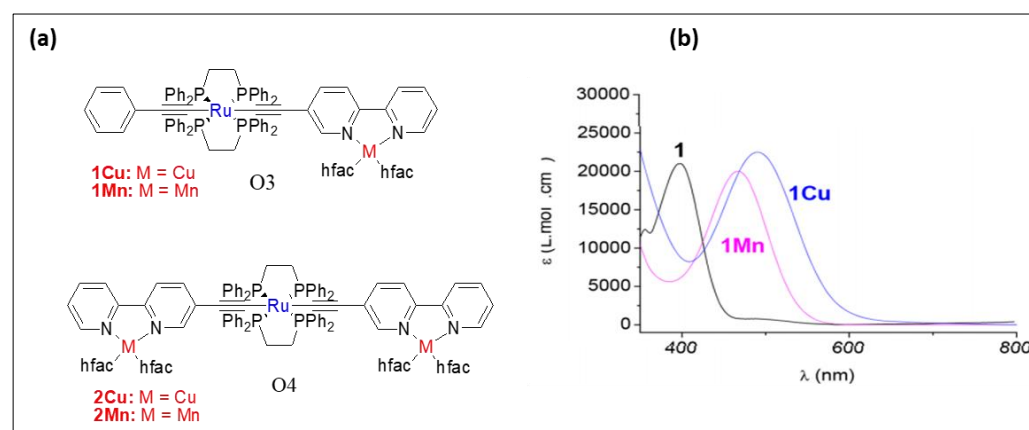


Figure 7. (a) Structures of bimetallic and trimetallic Ru/Cu and Ru/Mn complexes **O3** and **O4** and (b) the optical absorption spectra (in CH_2Cl_2) of **O3** when $M = \text{Cu}$ (**1Cu**) and $M = \text{Mn}$ (**1Mn**) along with the corresponding monometallic Ru-bipyridyl compound (**1**). Reprinted (adapted) with permission from Di Piazza, E.; Boilleau, C.; Vacher, A.; Merahi, K.; Norel, L.; Costuas, K.; Roisnel, T.; Choua, S.; Turek, P.; Rigaut, S., Ruthenium carbon-rich group as a redox-switchable metal coupling unit in linear trinuclear complexes. *Inorg. Chem.* 2017, 56, (23), 14540–14555. Copyright 2017 American Chemical Society.

In contrary to this, theoretical and experimental studies suggest that the two metal centers in binuclear heterometallic Ru(I)/Re(I) complexes **O5–O7** (Figure 8) are weakly coupled [27]. Chen et al. [26] found that the insertion of one or more heterometal (Re/Ru) reduces the π^* energy level in the ethynyl bipyridyl ligand in platinumynes and thus alters the photo-physical properties. For example, complexes (**O8** and **O9**, Figure 8) showed a red-shift in optical absorption and longer lifetime (in μs) compared to monometallic platinumynes (Table 2). Complex with Pt/Ru couple ($\lambda_{\text{max}}^{\text{abs}} = 504 \text{ nm}$, $\lambda_{\text{max}}^{\text{em}} = 658 \text{ nm}$ and $\tau_0 = < 0.1 \mu\text{s}$) showed red shifted absorption and emission compared to Pt/Re ($\lambda_{\text{max}}^{\text{abs}} = 427 \text{ nm}$, $\lambda_{\text{max}}^{\text{em}} = 595 \text{ nm}$ and $\tau_0 = < 1.5, 0.22 \mu\text{s}$) and Pt ($\lambda_{\text{max}}^{\text{abs}} = 392 \text{ nm}$, $\lambda_{\text{max}}^{\text{em}} = 540 \text{ nm}$ and $\tau_0 = < 0.1 \mu\text{s}$) complexes.

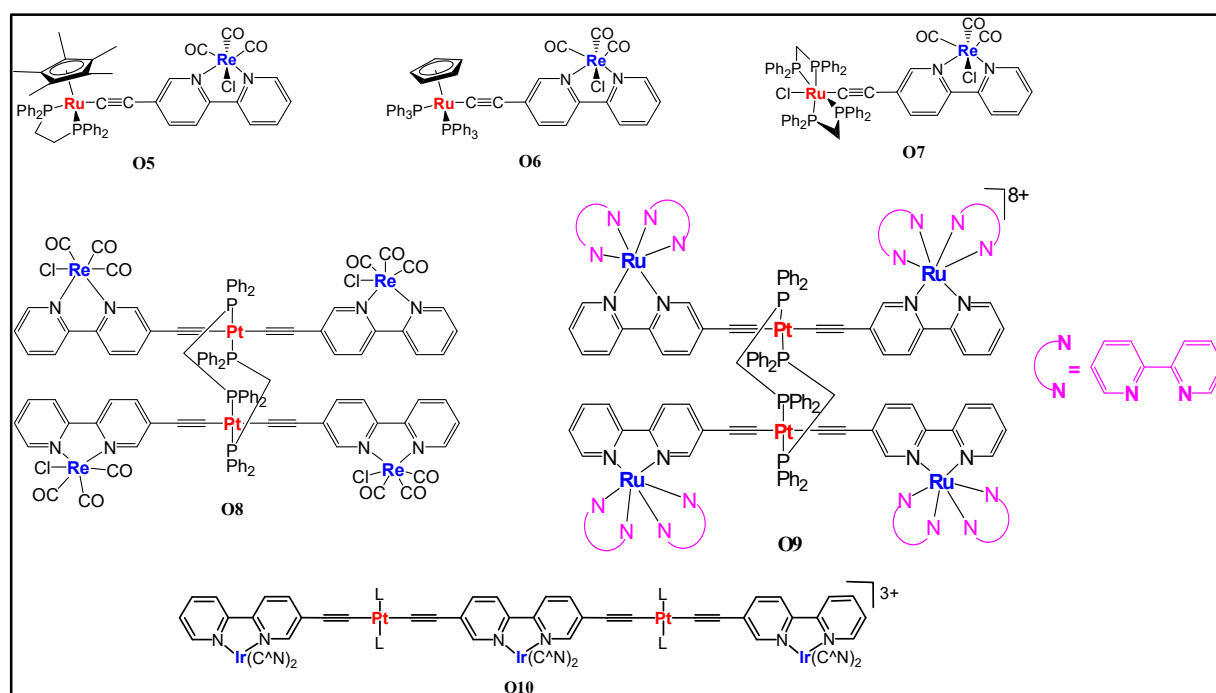


Figure 8. Structures of the *d-d* and *d-f* type heterometallic complexes O5–O10.

In addition to these small molecular systems, several polymeric complexes bearing *d-d* metal fragments were also investigated [53]. Complex O10 (Figure 8) is an example of a highly emissive (Table 2) pentanuclear complex containing Pt(II) and Ir(III) fragments [54]. An efficient triplet energy transfer between the terminal and central Ir(III) cores through the Pt(II) moiety was reported in such systems.

Table 2. Photoluminescence (PL) data of some selected heterometallic metalla-yne O1–O4 and O8–O10.

Code	Metals	λ_{abs} (nm)	λ_{ems} (nm)	Lifetime of S_1 (τ^a , μ s)	Lifetime of T_1 (τ^b , μ s)	Φ (%)	Ref.
O1 (R = Me)	Pd/Re	236, 284, 336sh, 416	628 ^a , 589 ^b	<0.1	0.73	-	[50]
O1 (R = H)	Pd/Re	238, 284, 334sh, 426	639 ^a , 594 ^b	<0.1	0.62	-	[50]
O2 (dppm)	Pd/Ru	386	-	-	-	-	[51]
O2 (dppe)	Pd/Ru	389	-	-	-	-	[51]
O3	Ru/Cu	308, 494	-	-	-	-	[52]
O3	Ru/Mn	308, 468	-	-	-	-	[52]
O4	Ru/Cu	308, 494	-	-	-	-	[52]
O4	Ru/Mn	306, 468	-	-	-	-	[52]
O8	Pt/Re	271, 382, 427	595	1.5, 0.22	-	0.0018	[26]
O9	Pt/Ru	243, 291, 360, 504	658	<0.1	-	0.045	[26]
O10	Pt/Ir	255, 315, 415, 435	560 ^a , 613 ^a , 663 ^a , 550 ^b , 595 ^b , 651 ^b	2.3	2.5, 1.9	3.3	[54]

λ_{abs} : absorption wavelength peaks, λ_{ems} : emission wavelength peaks, sh: shoulder, a: measured at 298 K, b: measured at 77 K, Φ : quantum yield.

Harvey and coworkers [55] prepared a series of mono- and bimetallic Pt(II)/Ir(III) complexes (P12–P14, Figure 9a) and assessed their photo-physical properties. The photophysical features of the heterometallic complexes were found to be a hybrid of the monometallic complexes used. For instance, Ir(III)-containing 5,5'-bisacetylide complex ($\Phi = 1.6\%$, $\tau = 0.09 \mu$ s) showed structureless emission maxima at 638 nm while Pt(II) dimer ($\Phi = 13.7\%$, $\tau = 39.2 \mu$ s) showed a blue-shifted structured emission at 561 nm. The introduction of a second luminescent fragment in Pt(II) complex ($\Phi = 13.7\%$, $\tau = 39.2 \mu$ s) led

to Pt/Ir ($\Phi = 4\%$, $\tau = 1.33 \mu\text{s}$) dimer with red-shifted emission at 623 nm. Under similar conditions, polymer **P13**, which is a Bipy containing Pt(II) poly-yne exhibits emission at 561 nm ($\Phi = 12.8\%$, $\tau = 9.2 \mu\text{s}$, Table 3). Ir-containing polymer **P12** showed emission at 617 nm ($\Phi = 2.6\%$, $\tau = 1.22 \mu\text{s}$, Table 3) (Figure 9b). Later the same group [56] compared the photo-physical and electrochemical properties of complex **P14** (Figure 9a). Upon fluorination of the pendant ligand, the nature of the excited state remains the same; however, there were some changes in the absorption and in emission profiles (Table 3).

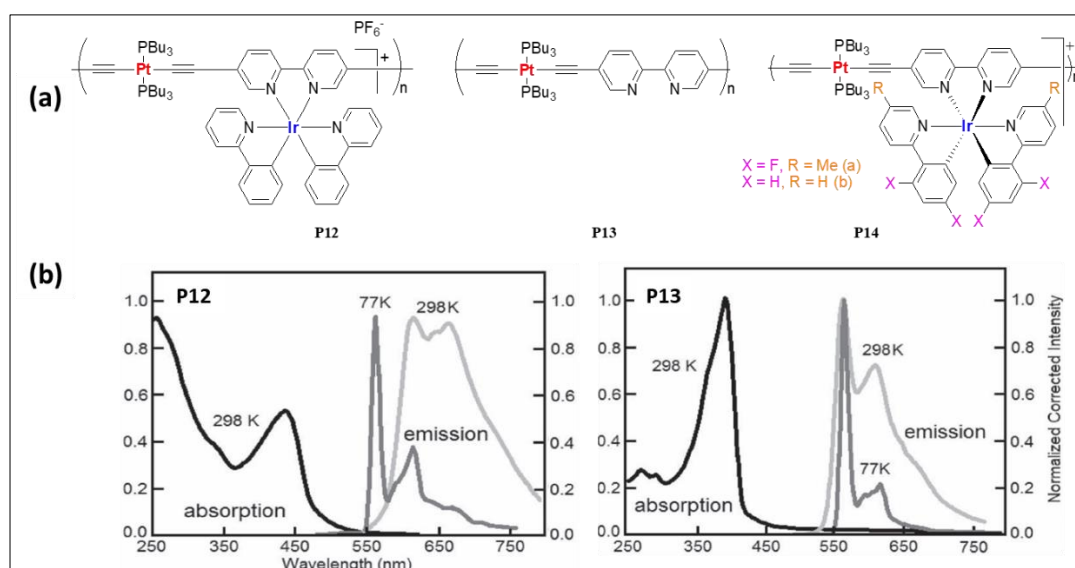


Figure 9. (a) Mono- and bi-metallic Pt(II)/Ir(III) polymers (**P12–P14**). (b) Absorption (298 K) and emission spectra of **P12** and **P13** at 298 and 77 K. Reproduced with permission from ref. [55].

In the past, we demonstrated that the topology of alkynylated π -conjugated ligands plays an important role in determining electron transfer and other processes [57]. For example, it was found that the Pt(II) acetylide attached to different positions of azobenzene [15] and stilbene [16] exhibit different levels of isomerization. Later, we found that the inclusion of Re(I) core in Pt(II) di-yne and poly-yne alters the optical properties of the complexes, the extent of which depends on the topology of the bipyridine (Bipy) ligand (i.e., 5,5'- or 6,6' systems, **P15–P16**, Figure 10 and Table 3) [33]. Like other reports, we also noted that the 5,5'-bisalkynyl systems are much better than the 6,6'- counterparts. Wong and co-workers [58] also reported that the coordination of a Re(I) unit, as well as the number of thienyl rings, plays a central role in determining the PL properties of poly(platina-yne) **P17** (Figure 10, Table 3).

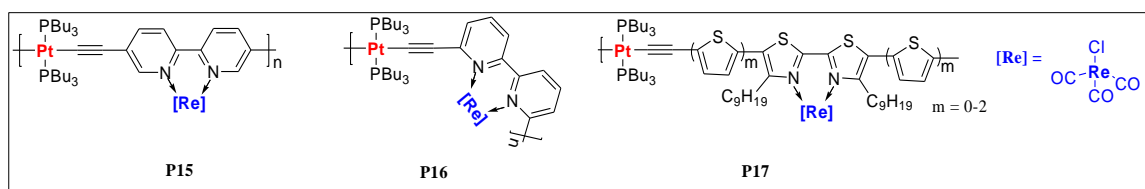


Figure 10. Re(I)-coordinated Pt(II) poly(metalla-yne)s.

Table 3. Photoluminescence (PL) data of selected heterometallic poly(metalla-ynes) **P12–P19**.

Code	Metals	Molecular Weight ($\times 10^4$)		λ_{abs} (nm)	λ_{ems} (nm)	Lifetime of S_1 (τ^a , ns)	Lifetime of T_1 , (τ^b , μ s)	Φ (%)	E_g (eV)	Ref.
		M_w	M_n							
P12	Pt/Ir	1.33	1.18	250, 280, 340, 435	617 ^a , 563 ^b	1220	5.67	2.60	-	[55]
P13	Pt	1.22	2.48	253, 270, 295, 390	561 ^a , 562 ^b	9200	70	12.80	-	[55]
P14a	Pt/Ir	-	-	250, 260, 315, 415, 485	628 ^a , 547 ^b , 592 ^b , 640 ^b	800	4.81	1.0	-	[56]
P14b	Pt/Ir	-	-	250, 280, 340, 435	555 ^a , 617 ^a , 655 ^a , 558 ^b , 596 ^b , 654 ^b	2500, 1900	5.7, 3.3	2.6	-	[56]
P15	Pt/Re	6.1	7.7	343, 419, 448	-	-	-	-	-	[33]
P16	Pt/Re	5.5	8.3	276, 300, 324, 388, 402	-	-	-	-	-	[33]
P17 (m = 0)	Pt/Re	1.3	3.8	230, 306, 539	582 ^a	0.22	-	0.05	2.18	[58]
P17 (m = 1)	Pt/Re	1.0	1.9	229, 362, 548	659 ^a	0.44	-	0.19	1.95	[58]
P17 (m = 2)	Pt/Re	0.9	1.9	229, 400, 552	729 ^a	0.34	-	0.10	1.85	[58]
P18	Pt/Ir	1.3	-	229, 260, 287, 379, 400, 446, 465, 487	549 ^a , 588 ^a , 552 ^b , 599 ^b	110	10.82	12.3	2.44	[49]
P19	Pt/Ir	1.1×10^4	-	229, 251, 283, 383, 400, 474, 502	577 ^a , 625 ^a , 577 ^b , 631 ^b	510	12.12	4.80	2.39	[49]

M_w : average weight molecular weight, M_n : number weight molecular weight, λ_{abs} : absorption wavelength peaks, λ_{ems} : emission wavelength peaks, sh: shoulder, a: measured at 298 K, b: measured at 77 K, Φ : quantum yield, E_g : energy gap.

2.2.2. *d-f* Metal-Containing Systems

In contrast to *d*-block elements, *f*-block lanthanides (Ln) display fascinating optical (colorful sharp line-like emission spectra with large Stokes shifts and long lifetime) and magnetic properties [32,59–61]. Owing to these features, they serve as an excellent dopant for the fabrication of display devices and probes for cellular imaging. However, it is often overshadowed by the low molar absorption coefficients ($\epsilon \sim 0.1\text{--}10 \text{ M}^{-1}\cdot\text{cm}^{-1}$) of Ln(III) complexes as *f-f* electronic transitions are forbidden by parity and spin selection rules. To overcome this limitation, coordination of transition metal organometallic complexes was proposed as it would facilitate efficient electronic energy transfer (EET) via the *antenna effect* [62–66]. In addition to the synergistic effect of these different blocks of metals, judicious selection of coordinating ligand, the excitation wavelength could be extended to the visible region [64]. In this context, π -conjugated arylethynyl spacer covalently linked to transition metal is an excellent choice [67–69]. Exploiting this concept, several hetero-multimetallc Ln(III) complexes incorporating Pt(II) acetylide chromophore were reported [25,32,34]. It was noted that Pt(II) acetylide complex strongly sensitizes the Ln(III) in the Vis-NIR region with a high Φ_f value [66,70]. In complexes (**O11–O17**, Figure 11, Table 4), an efficient energy transfer to Ln(III) ions takes place and the separation between Pt—Ln played an important role [28,71–73]. Regardless of Pt(II) isomer configuration (*cis* or *trans*) the low energy phosphorescence from $d\pi_{(Pt)} \rightarrow \pi^*(C\equiv C-Bipy/phen)^3MLCT$ excited states were quenched indicating efficient energy transfer from the Pt(II) acetylide chromophore to lanthanide centers.

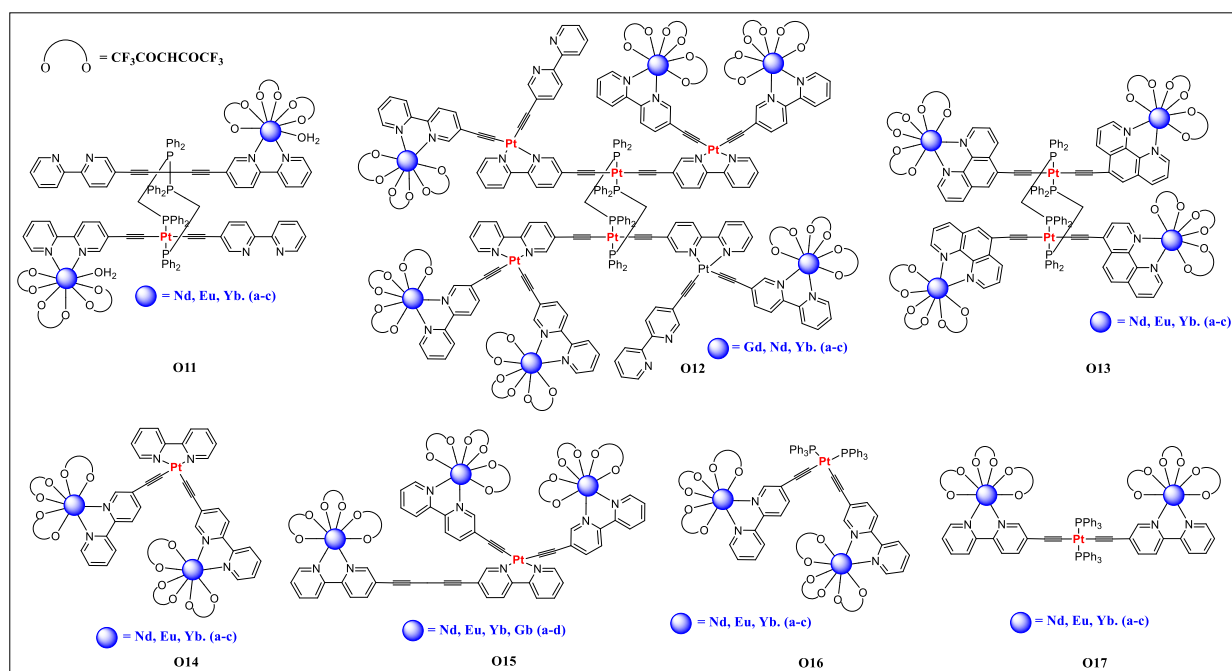


Figure 11. Acetylide-functionalized diimine-based hetero-multimetallic complexes with different lanthanides metal ions (O11–O17).

Belayev and coworkers [74] reported Au(I)/Eu(III)-based dually luminescent D- π -A type complexes O18–O20 (Figure 12a) with solvatochromic features (Figure 12b). In these heterometallic complexes, different π -extended phosphines ligands attached to Au(I) center were tested. It was noted that the partial energy transfer from phosphine \rightarrow Eu(III) and efficient energy transfer from β -diketonate \rightarrow Eu(III) were the main causes of dual emission (Table 4).

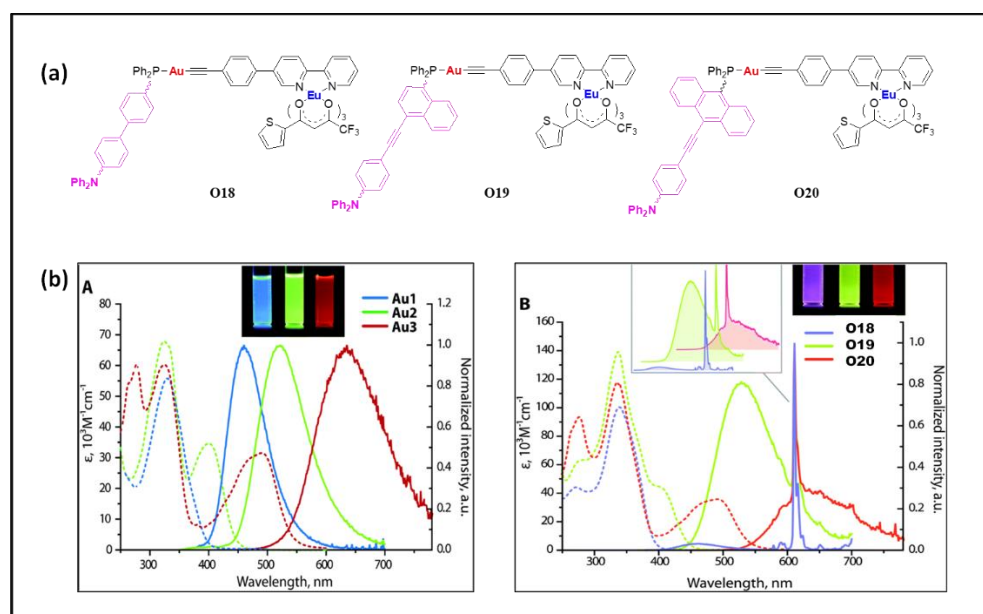


Figure 12. (a) Bipyridine-based Au(I) complexes incorporating Eu(III) β -diketonate fragment. (b) UV-vis absorption (dashed lines) and normalized emission (solid lines) spectra of metallo-ligands Au1–Au3 (A), and dyads O18–O20 (B) the photographs show the corresponding solutions under UV light. Reproduced from ref. [74] licensed under a Creative Commons Attribution Non-Commercial 3.0 Unported License.

We recently investigated the structural and optical properties of Bipy-based Pt(II)/Eu(III) heterometallic complexes **O21** and **O22** (Figure 13, Table 4) [32,34]. In line with the other studies, we also found an efficient, but topology-dependent, $d \rightarrow f$ energy transfer in the complexes. Whereas complex **O21** exhibited typical Eu(III)-based red emission, complex **O22** displayed dual emission (red and green) with excitation in both the UV and Vis regions. Moreover, complexes exhibited longer lifetime (τ_{obs}) than similar complexes reported in the literature [28,75].

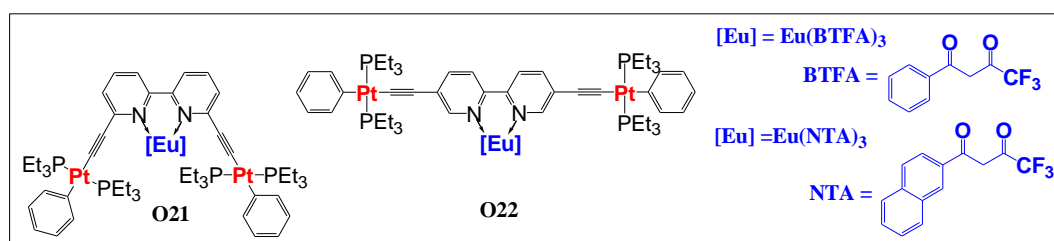


Figure 13. “ d - f ” type Eu(III)-co-ordinated Pt(II) di-ynes.

Table 4. Photoluminescence data of heterometallic metalla-ynes **O11**–**O22** and **O24**–**O29**.

Code	Metals	λ_{abs} (nm)	λ_{ems} (nm)	Lifetime of S_1 (τ^a , μs)	Φ (%)	Ref.
O11a	Pt/Nd	-	1060 ^a	-	0.84	[28]
O11b	Pt/Eu	-	615 ^a	250.60	24	[28]
O11c	Pt/Yb	-	980	12.20	5.65	[28]
O12a	Pt/Gd	-	563	0.84	0.07	[71]
O12b	Pt/Nd	-	1060	weak	-	[71]
O12c	Pt/Yb	-	980	12.10	0.061	[71]
O13a	Pt/Nd	-	1060	-	0.2	[28]
O13b	Pt/Eu	-	615	33.60	0.5	[28]
O13c	Pt/Yb	-	980	12.90	0.635	[28]
O14a	Pt/Nd	304, 320, 363, 401	1061	-	-	[72]
O14b	Pt/Eu	301, 323, 365, 400	613	105	5.4	[72]
O14c	Pt/Yb	295, 322, 365, 400	980	11.8	6.3	[72]
O15a	Pt/Nd	304, 329, 358, 381, 430	1060	-	-	[72]
O15b	Pt/Eu	299, 329, 357, 382, 430	613	164	1.7	[72]
O15c	Pt/Yb	294, 328, 357, 382, 430	980	10.9	0.54	[72]
O15d	Pt/Gd	303, 329, 358, 383, 430	572	0.40	2.4	[72]
O16a	Pt/Nd	228, 297, 371	423, 1061	<0.01	-	[73]
O16b	Pt/Eu	228, 303, 375	420, 613	<0.01, 109.5	1.4	[73]
O16c	Pt/Yb	228, 297, 371	428, 980	<0.01, 12.6	0.63	[73]
O17a	Pt/Nd	229, 305, 372	421, 1060	<0.01	-	[73]
O17b	Pt/Eu	230, 303, 375	415, 613	<0.01, 216.3	1.0	[73]
O17c	Pt/Yb	228, 293, 384	448, 980	<0.01, 12.7	0.64	[73]
O18	Au/Eu	271, 339	460, 580, 592, 611, 654, 700	0.0022, 280.00	15	[74]
O19	Au/Eu	280, 337, 404	525, 611	0.0017, 434.00	21	[74]
O20	Au/Eu	276, 336, 495	611, 635, 705	0.0041, 404.10	16	[74]
O21	Pt/Eu	325	550–725	590	54	[32]
O21	Pt/Eu	325	550–725	410	29	[32]
O22	Pt/Eu	416	425–531, 550–725	39.52, 519.86	39	[34]
O24	Ir/Eu	242, 283, 343	578, 590, 615, 684, 697	0.780, 0.116, 0.51, 0.095	-	[76]
O24	Ir/Gd	242, 285, 338	560	1.1, 0.45, 0.64, 0.22	4.8	[76]
O25	Ir/Eu	241, 292, 357	616	1.24, 0.168	-	[76]
O25	Ir/Gd	242, 292, 358	595	1.26, 0.233	2.6	[76]

Table 4. Cont.

Code	Metals	λ_{abs} (nm)	λ_{ems} (nm)	Lifetime of S ₁ (τ^a , μ s)	Φ (%)	Ref.
O26	Au/Re	243, 265, 305, 366	592	-	-	[77]
O27	Au/Re	240, 278, 3.19, 357	576	-	-	[77]
O28	Au/Re	237, 271, 318, 352	607	-	-	[77]
O29	Au/Re	368	614	1060	30.4	[69]

λ_{abs} : absorption wavelength peaks, λ_{ems} : emission wavelength peaks, sh: shoulder, τ^a : lifetime measured at 298 K, Φ : quantum yield.

3. Applications

It is clear from the above discussion that the optical properties of homo- and heterometallic metalla-ynes and poly(metalla-ynes) are highly sensitive to the type of metal ions, number of π -linkages, spacers and end-groups. Despite this knowledge, relatively less attention has been focused on application-oriented studies. From the application point of view, complex O23 (Figure 14) is the first example of a heterometallic complex featuring an NLO response [78]. This complex was reported to be a two-photon absorber (2PA) as well as an excited-state absorber under two different conditions. Heterometallic polymers (P1–P3, Figure 2) were reported as promising OPL candidates [47]. Among the tested heterometallic poly(metalla-ynes), Hg(II)/Pt(II) exhibit best optical-limiting thresholds ($0.07 \text{ J}\cdot\text{cm}^{-2}$ at 92% linear transmittance) followed by Pd/Pt ($0.35 \text{ J}\cdot\text{cm}^{-2}$) and Pd/Hg ($0.75 \text{ J}\cdot\text{cm}^{-2}$) couples. On the other hand, polymers P18 and P19 (Figure 14) are promising materials for the fabrication of phosphorescent organic light-emitting diodes (PHOLEDs) [49]. Both polymers can effectively absorb energy from the host properly, which is one of the prerequisites to realize high-performance OLED devices. Both polymers showed high performance (luminance = 2708 and $3356 \text{ c}\cdot\text{dm}^{-2}$, EQE = 0.5% and 0.67%, luminance efficiency = 0.6 and $0.55 \text{ L}\cdot\text{mW}^{-1}$ for P18 and P19, respectively) with orange-yellow color emission at 10% doping level.

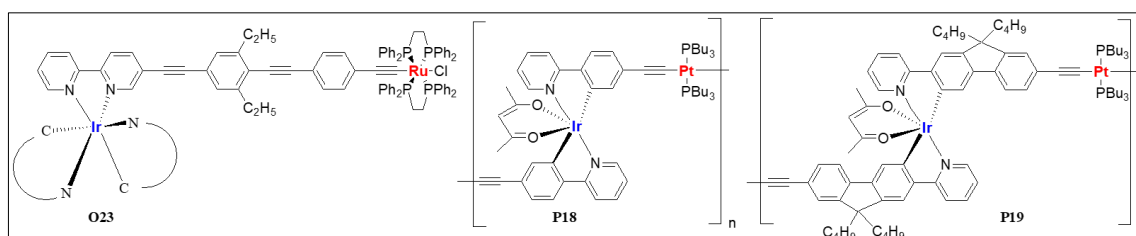


Figure 14. Heterometallic poly-ynes (O23, P18 and P19) for NLO and OLED applications.

The application of luminescent lanthanide complexes for dual imaging (magnetic resonance imaging and optical imaging) is well established [79]. Jana and co-workers [76] showed that merging the high relaxivity feature of lanthanide ions with the luminescence from the Ir(III)/Ln(III) centers is an intriguing way to produce highly efficient bioimaging probes. The reported heterometallic complexes with $d \rightarrow f$ energy transfer feature exhibit high aqueous solubility, high intake in cancerous cell lines, low toxicity, and lysosomal target ability. Moreover, it was also reported that dinuclear complexes (O24, Figure 15a) were better than their trinuclear counterparts (O25, Figure 15a). One of the reported dinuclear complexes (O24: Ln = Gd) showed multi-modal imaging capability, which is the first of its kind. The luminescence lifetime of this multi-modal imaging probe varies inversely with the concentration of O₂ (Figure 15b).

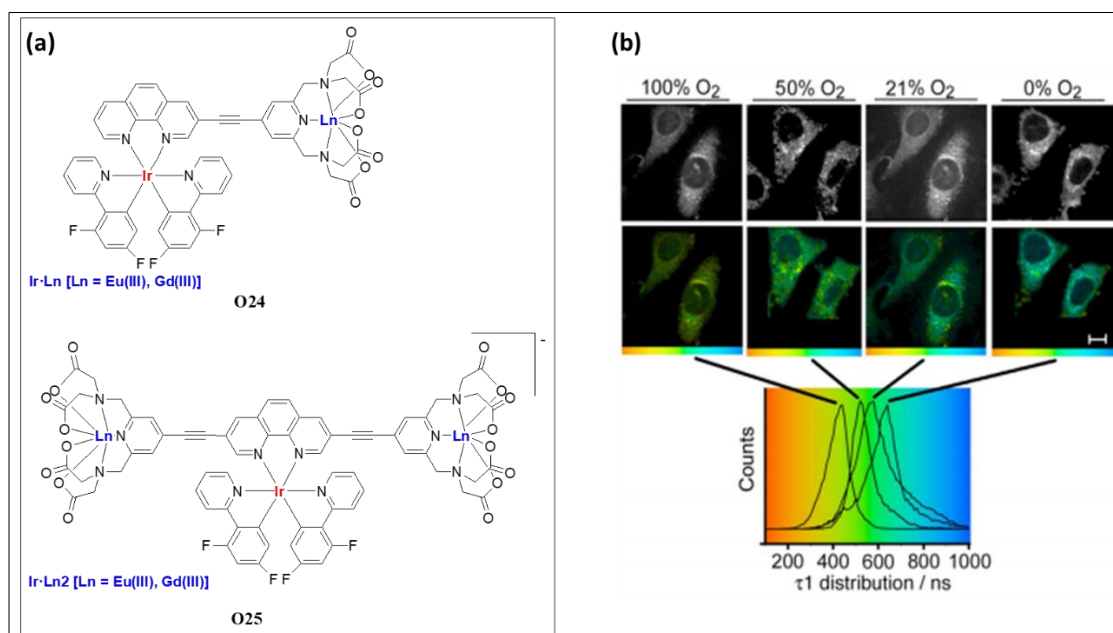


Figure 15. (a) Ir(III)/Ln(III) di- and trinuclear complexes (**O24** and **O25**). (b) Two-photon PLIM imaging of **O24** (Ln = Gd) stained HeLa cells under different concentrations of oxygen. Reproduced with permission from ref. [76].

On the contrary, nucleus and nucleolus localizing ability was reported for heterometallic Re(I)/Au(I) complexes (**O26–O28**, Figure 16) [77]. Compared to monometallic complexes ($IC_{50} = 120\text{--}200\ \mu\text{m}$), higher cytotoxicity was exerted by the heterometallic derivatives ($IC_{50} = 4.4\text{--}19\ \mu\text{m}$).

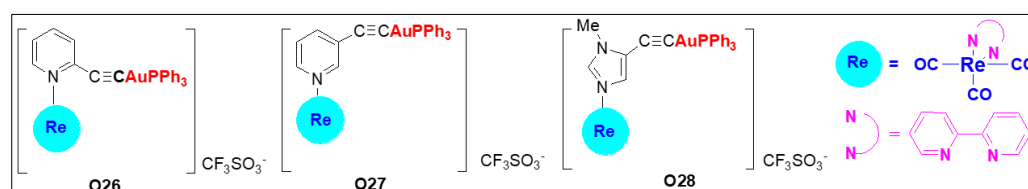


Figure 16. Heterometallic Re(I)/Au(I) complexes (**O26–O28**) with potential for cell imaging and cancer therapy.

Researchers also explored the pesticides/chirality sensing ability of heterometallic complexes. Zhu and coworkers [80] exploited the luminescent enhancement by post-assembly modification of complex **O29** (Figure 17) for the sensing of some common pesticides. They reported that self-assembled coordination-driven complexes show a high propensity for thiophosphonates (OMA, MET and MAL) and turn-on the luminescence via displacement mechanism leading to intensity enhancement (~ 4 -fold). However, negligible responses were noted for other pesticides. Overall, heterometallic complexes with open metal sites offer a new design principle in constructing sensors. Very recently, heterometal-organic macrocycles were also reported as having the ability to detect enantiomeric excess (ee) [81].

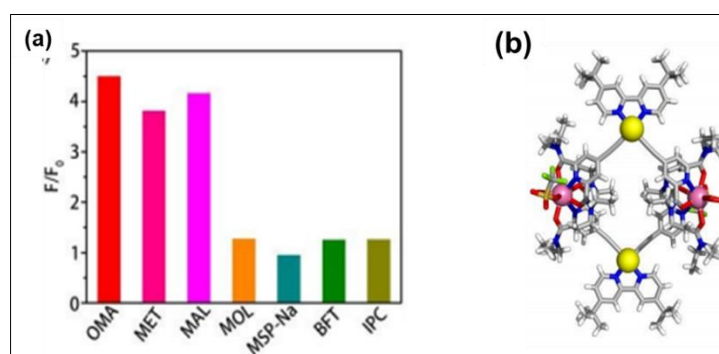


Figure 17. (a) Luminescence response to various pesticides, and (b) X-ray crystal structure of **O29** (C, gray; H, white; N, blue; O, red; S, orange; F, light green; Pt, yellow; Eu, pink). Reproduced with permission from ref. [80].

4. Conclusions

In summary, we reviewed the structure, properties and applications of metalla-ynes and poly(metalla-ynes) containing one or more types of metal ions. Both *d-d* and *d-f* combinations (either in the main- or side-chain) were briefly summarized. To date, a number of luminescent materials that contain *d-d* and *d-f* combinations (either in the main- or side-chain) separated by mono-, oligo- and poly-ynes have been developed and studied. From the discussion, it is quite clear that the combination of two metal centers, especially transition and lanthanide metals, is an effective way to modulate the PL properties. In the majority of cases, transfer of energy takes place from transition metal to lanthanide core, hence enhancing the luminescence intensity. Often, the hybrid material exhibits luminescence properties in between the transition and the lanthanide metal. In addition, owing to the wide variety of auxiliary groups, solution-processable small and large macromolecules can be realized with applications ranging from OLEDs through sensing to imaging. Despite multiple advantages, challenges such as limited synthesis incorporating metals other than the discussed ones, a mixture of products, batch-to-batch variation in the performance especially for polymeric materials are some of the main obstacles in this field.

Author Contributions: Conceptualization, A.H. and M.S.K.; writing—original draft preparation, R.A.A.-B.; I.J.A.-B. and H.A.-S.; visualization, H.A.-S. and R.A.A.-B.; supervision, M.S.K.; writing—reviewing and editing A.H. and M.S.K. All authors have read and agreed to the published version of the manuscript.

Funding: This research was funded by Ministry of Higher Education, Research, and Innovation (MoHERI) grant number [RC/RG-SCI/CHEM/20/01].

Institutional Review Board Statement: Not applicable.

Informed Consent Statement: Not applicable.

Data Availability Statement: Not applicable.

Acknowledgments: RAA acknowledges A'Sharqiyah University for a collaborative research visit to SQU. MSK acknowledges the Ministry of Higher Education, Research, and Innovation (MoHERI), Oman for support (Grant No. RC/RG-SCI/CHEM/20/01). The authors thank Khalid Al Hashimi of the Department of Basic Sciences, College of Applied and Health Sciences, A'Sharqiyah University, Ibra, Oman, for his help in editing the graphical abstract.

Conflicts of Interest: The authors declare no conflict of interest.

Abbreviations

acac	Acetylacetone
Bipy	Bipyridine
D-A	Donor-acceptor
EET	Electronic energy transfer
EQE	External quantum efficiency
E_g	Energy gap
GPC	Gel permeation chromatography
HOMO	Highest occupied molecule orbital
ISC	Inter system crossing
Ln(III)	Trivalent lanthanide
LUMO	Lowest unoccupied molecular orbital
MLCT	Metal to ligand charge transfer
M_n	Number average molecular weight
M_w	Weight average molecular weight
NLO	Non-linear optical
NMR	Nuclear magnetic resonance
O-E	Optoelectronic
OLEDs	Organic light-emitting diodes
OPL	Optical power limiting
phen	Phenyl
PHOLEDs	Phosphorescent organic light-emitting diodes
PL	Photo-luminescence
PLQY	Photo-luminescence quantum yields
RT	Room-temperature
SOC	Spin-orbit coupling
THF	Tetrahydrofuran
UV	Ultraviolet
Vis	Visible
τ	lifetime
ϕ	Quantum yield
ϵ	Absorption coefficient
λ_{max}^{em}	Wavelength of maximum emission
λ_{max}^{abs}	Wavelength of maximum absorption

References

1. Haque, A.; Al-Balushi, R.A.; Al-Busaidi, I.J.; Khan, M.S.; Raithby, P.R. Rise of Conjugated poly-ynes and poly(metalla-ynes): From design through synthesis to structure–property relationships and applications. *Chem. Rev.* **2018**, *118*, 8474–8597. [[CrossRef](#)] [[PubMed](#)]
2. Haque, A.; Xu, L.; Al-Balushi, R.A.; Al-Suti, M.K.; Ilmi, R.; Guo, Z.; Khan, M.S.; Wong, W.-Y.; Raithby, P.R. Cyclometallated tridentate platinum(II) arylacetylide complexes: Old wine in new bottles. *Chem. Soc. Rev.* **2019**, *48*, 5547–5563. [[CrossRef](#)] [[PubMed](#)]
3. Ho, C.-L.; Yu, Z.-Q.; Wong, W.-Y. Multifunctional polymetallaynes: Properties, functions and applications. *Chem. Soc. Rev.* **2016**, *45*, 5264–5295. [[CrossRef](#)]
4. Dong, Q.; Meng, Z.; Ho, C.-L.; Guo, H.; Yang, W.; Manners, I.; Xu, L.; Wong, W.-Y. A molecular approach to magnetic metallic nanostructures from metallopolymer precursors. *Chem. Soc. Rev.* **2018**, *47*, 4934–4953. [[CrossRef](#)]
5. Al-Busaidi, I.J.; Haque, A.; Al Rasbi, N.K.; Khan, M.S. Phenothiazine-based derivatives for optoelectronic applications: A review. *Synth. Met.* **2019**, *257*, 116189. [[CrossRef](#)]
6. Rausch, A.F.; Homeier, H.H.H.; Yersin, H. Organometallic Pt(II) and Ir(III) triplet emitters for oled applications and the role of spin–orbit coupling: A study based on high-resolution optical spectroscopy. In *Photophysics of Organometallics*; Lees, A.J., Ed.; Springer: Berlin/Heidelberg, Germany, 2010; pp. 193–235.
7. Yersin, H. *Highly Efficient OLEDs with Phosphorescent Materials*; Wiley-VCH Verlag: Weinheim, Germany; p. 2008.
8. Wilson, J.S.; Köhler, A.; Friend, R.H.; Al-Suti, M.K.; Al-Mandhary, M.R.A.; Khan, M.S.; Raithby, P.R. Triplet states in a series of Pt-containing ethynylenes. *J. Chem. Phys.* **2000**, *113*, 7627–7634. [[CrossRef](#)]
9. Wilson, J.S.; Chawdhury, N.; Al-Mandhary, M.R.A.; Younus, M.; Khan, M.S.; Raithby, P.R.; Köhler, A.; Friend, R.H. The energy gap law for triplet states in Pt-containing conjugated polymers and monomers. *J. Am. Chem. Soc.* **2001**, *123*, 9412–9417. [[CrossRef](#)] [[PubMed](#)]

10. Stefko, M.; Tzirakis, M.D.; Breiten, B.; Ebert, M.O.; Dumele, O.; Schweizer, W.B.; Gisselbrecht, J.P.; Boudon, C.; Beels, M.T.; Biaggio, I.; et al. Donor-acceptor (D-A)-substituted polyynes chromophores: Modulation of their optoelectronic properties by varying the length of the acetylene spacer. *Chemistry* **2013**, *19*, 12693–12704. [[CrossRef](#)] [[PubMed](#)]
11. Köhler, A.; Younus, M.; Al-Mandhary, M.R.A.; Raithby, P.R.; Khan, M.S.; Friend, R.H. Donor-acceptor interactions in organometallic and organic polyynes. *Syn. Metals* **1999**, *101*, 246–247. [[CrossRef](#)]
12. Jimenez, A.J.; Sekita, M.; Caballero, E.; Luisa Marcos, M.; Salome Rodriguez-Morgade, M.; Guldi, D.M.; Torres, T. Assembling a phthalocyanine and perylene diimide donor-acceptor hybrid through a Platinum(II) diacetylide linker. *Chem. -Eur. J.* **2013**, *19*, 14506–14514. [[CrossRef](#)]
13. Shizu, K.; Lee, J.; Tanaka, H.; Nomura, H.; Yasuda, T.; Kaji, H.; Adachi, C. Highly efficient electroluminescence from purely organic donor-acceptor systems. *Pure Appl. Chem.* **2015**, *87*, 627–638. [[CrossRef](#)]
14. Cekli, S.; Winkel, R.W.; Schanze, K.S. Effect of Oligomer Length on Photophysical Properties of Platinum Acetylide Donor-Acceptor-Donor Oligomers. *J. Phys. Chem. A* **2016**, *120*, 5512–5521. [[CrossRef](#)]
15. Al-Balushi, R.A.; Haque, A.; Jayapal, M.; Al-Suti, M.K.; Husband, J.; Khan, M.S.; Skelton, J.M.; Molloy, K.C.; Raithby, P.R. Impact of the alkyne substitution pattern and metalation on the photoisomerization of azobenzene-based Platinum(II) diynes and polyynes. *Inorg. Chem.* **2016**, *55*, 10955–10967. [[CrossRef](#)]
16. Al-Busaidi, I.J.; Haque, A.; Husband, J.; Al Rasbi, N.K.; Abou-Zied, O.K.; Al Balushi, R.; Khan, M.S.; Raithby, P.R. Electronic and steric effects of platinum (ii) di-yne and poly-yne substituents on the photo-switching behaviour of stilbene: Experimental and theoretical insights. *Dalton Trans.* **2021**, *50*, 2555–2569. [[CrossRef](#)]
17. Wong, W.-Y.; Ho, C.-L. Di-, oligo- and polymetallaynes: Syntheses, photophysics, structures and applications. *Coord. Chem. Rev.* **2006**, *250*, 2627–2690. [[CrossRef](#)]
18. Haque, A.; Al-Balushi, R.A.; Khan, M.S. σ -Acetylide complexes for biomedical applications: Features, challenges and future directions. *J. Organomet. Chem.* **2019**, *897*, 95–106. [[CrossRef](#)]
19. Al-Rasbi, N.K.; Derossi, S.; Sykes, D.; Faulkner, S.; Ward, M.D. Bimetallic Pt (II)-bipyridyl-diacetylide/Ln (III) tris-diketonate adducts based on a combination of coordinate bonding and hydrogen bonding between the metal fragments: Syntheses, structures and photophysical properties. *Polyhedron* **2009**, *28*, 227–232. [[CrossRef](#)]
20. Lazarides, T.; Sykes, D.; Faulkner, S.; Barbieri, A.; Ward, M.D. On the mechanism of d-f energy transfer in Ru^{II}/Ln^{III} and Os^{II}/Ln^{III} dyads: Dexter-type energy transfer over a distance of 20 Å. *Chem. Eur. J.* **2008**, *14*, 9389–9399. [[CrossRef](#)] [[PubMed](#)]
21. Judkins, E.C.; Zeller, M.; Ren, T. Synthesis and characterizations of macrocyclic Cr (III) and Co (III) 1-ethynyl naphthalene and 9-ethynyl anthracene complexes: An investigation of structural and spectroscopic properties. *Inorg. Chem.* **2018**, *57*, 2249–2259. [[CrossRef](#)] [[PubMed](#)]
22. Tian, Z.; Yang, X.; Liu, B.; Zhong, D.; Zhou, G.; Wong, W.-Y. New heterobimetallic Au (I)-Pt (II) polyynes achieving a good trade-off between transparency and optical power limiting performance. *J. Mater. Chem. C* **2018**, *6*, 11416–11426. [[CrossRef](#)]
23. Xu, L.; Ho, C.-L.; Liu, L.; Wong, W.-Y. Molecular/polymeric metallaynes and related molecules: Solar cell materials and devices. *Coord. Chem. Rev.* **2017**, *373*, 233–257. [[CrossRef](#)]
24. Li, H.; Xie, C.; Lan, R.; Zha, S.; Chan, C.-F.; Wong, W.-Y.; Ho, K.-L.; Chan, B.D.; Luo, Y.; Zhang, J.-X.; et al. A Smart Europium-Ruthenium complex as anticancer prodrug: Controllable drug release and real-time monitoring under different light excitations. *J. Med. Chem.* **2017**, *60*, 8923–8932. [[CrossRef](#)]
25. Xu, H.-B.; Deng, J.-G.; Kang, B. Designed synthesis and photophysical properties of multifunctional hybrid lanthanide complexes. *RSC Adv.* **2013**, *3*, 11367–11384. [[CrossRef](#)]
26. Xu, H.-B.; Zhang, L.-Y.; Chen, Z.-N. Syntheses, characterization and luminescence of Pt-M (M=Re, Ru, Gd) heteronuclear complexes with 5-ethynyl-2,2'-bipyridine. *Inorg. Chim. Acta* **2007**, *360*, 163–169. [[CrossRef](#)]
27. Koutsantonis, G.A.; Low, P.J.; Mackenzie, C.F.; Skelton, B.W.; Yufit, D.S. Coordinating Tectons: Bimetallic Complexes from bipyridyl terminated group 8 alkynyl complexes. *Organometallics* **2014**, *33*, 4911–4922. [[CrossRef](#)]
28. Xu, H.-B.; Shi, L.-X.; Ma, E.; Zhang, L.-Y.; Wei, Q.-H.; Chen, Z.-N. Diplatinum alkynyl chromophores as sensitizers for lanthanide luminescence in Pt₂Ln₂ and Pt₂Ln₄ (Ln=Eu, Nd, Yb) arrays with acetylide-functionalized bipyridine/phenanthroline. *Chem. Commun.* **2006**, 1601–1603. [[CrossRef](#)]
29. Torelli, S.; Imbert, D.; Cantuel, M.; Bernardinelli, G.H.; Delahaye, S.; Hauser, A.; Bünzli, J.-C.G.; Piguet, C. Tuning the decay time of lanthanide-based near infrared luminescence from micro-to milliseconds through d-f energy transfer in discrete heterobimetallic complexes. *Chem. -Eur. J.* **2005**, *11*, 3228–3242. [[CrossRef](#)]
30. Haque, A.; El Moll, H.; Alenezi, K.M.; Khan, M.S.; Wong, W.-Y. Functional materials based on cyclometalated platinum (II) β -diketonate complexes: A Review of structure-property relationships and applications. *Materials* **2021**, *14*, 4236. [[CrossRef](#)] [[PubMed](#)]
31. Ronson, T.K.; Lazarides, T.; Adams, H.; Pope, S.J.; Sykes, D.; Faulkner, S.; Coles, S.J.; Hursthouse, M.B.; Clegg, W.; Harrington, R.W.; et al. Luminescent Pt^{II} (bipyridyl)(diacetylide) chromophores with pendant binding sites as energy donors for sensitised near-infrared emission from lanthanides: Structures and photophysics of Pt^{II}/Ln^{III} assemblies. *Chem.-A Euro. J.* **2006**, *12*, 9299–9313. [[CrossRef](#)]
32. Ilimi, R.; Haque, A.; Al-Busaidi, I.J.; Al Rasbi, N.K.; Khan, M.S. Synthesis and photophysical properties of hetero trinuclear complexes of tris β -diketonate Europium with organoplatinum chromophore. *Dye. Pigment.* **2019**, *162*, 59–66. [[CrossRef](#)]

33. Haque, A.; Al-Balushi, R.; Al-Busaidi, I.J.; Al-Rasbi, N.K.; Al-Bahri, S.; Al-Suti, M.K.; Abou-Zied, O.K.; Khan, M.S.; Skelton, J.M.; Raithby, P.R. Two is better than one? Investigating the effect of incorporating Re(CO)₃Cl Side-chains into Pt(II) di-yne and poly-yne. *Inorg. Chem.* **2021**, *60*, 745–759. [[CrossRef](#)]
34. Al-Busaidi, I.J.; Ilmi, R.; Dutra, J.D.; Oliveira, W.F.; Haque, A.; Al Rasbi, N.K.; Marken, F.; Raithby, P.R.; Khan, M.S. Utilization of a Pt(II) di-yne Chromophore incorporating a 2,2'-bipyridine-5,5'-diyl spacer as a chelate to synthesize a green and red emitting d-f-d heterotrinnuclear complex. *Dalton Trans.* **2021**, *50*, 1465–1477. [[CrossRef](#)]
35. Beer, P.D.; Szemes, F.; Passaniti, P.; Maestri, M. Luminescent Ruthenium (II) bipyridine– Calix [4] arene complexes as receptors for lanthanide cations. *Inorg. Chem.* **2004**, *43*, 3965–3975. [[CrossRef](#)] [[PubMed](#)]
36. Glover, P.B.; Ashton, P.R.; Childs, L.J.; Rodger, A.; Kercher, M.; Williams, R.M.; De Cola, L.; Pikramenou, Z. Hairpin-shaped heterometallic luminescent lanthanide complexes for DNA intercalative recognition. *J. Am. Chem. Soc.* **2003**, *125*, 9918–9919. [[CrossRef](#)] [[PubMed](#)]
37. Klink, S.I.; Keizer, H.; van Veggel, F.C. Transition metal complexes as photosensitizers for near-infrared lanthanide luminescence. *Angew. Chem.* **2000**, *39*, 4319–4321. [[CrossRef](#)]
38. Zhang, X.; Hou, Y.; Xiao, X.; Chen, X.; Hu, M.; Geng, X.; Wang, Z.; Zhao, J. Recent development of the transition metal complexes showing strong absorption of visible light and long-lived triplet excited state: From molecular structure design to photophysical properties and applications. *Coord. Chem. Rev.* **2020**, *417*, 213371. [[CrossRef](#)]
39. Li, K.; Chen, Y.; Wang, J.; Yang, C. Diverse emission properties of transition metal complexes beyond exclusive single phosphorescence and their wide applications. *Coord. Chem. Rev.* **2021**, *433*, 213755. [[CrossRef](#)]
40. Long, N.J.; Williams, C.K. Metal alkynyl sigma complexes: Synthesis and materials. *Angew. Chem.* **2003**, *42*, 2586–2617. [[CrossRef](#)]
41. Packheiser, R.; Ecorchard, P.; Ruffer, T.; Lang, H. Heterometallic transition metal complexes based on unsymmetrical platinum (II) bis-acetylides. *Organometallics* **2008**, *27*, 3534–3546. [[CrossRef](#)]
42. Sonogashira, K.; Ohga, K.; Takahashi, S.; Hagihara, N. Studies of poly-yne polymers containing transition metals in the main chain. *J. Organomet. Chem.* **1980**, *188*, 237–243. [[CrossRef](#)]
43. Sonogashira, K.; Kataoka, S.; Takahashi, S.; Hagihara, N. Studies of poly-yne polymers containing transition metals in the main chain: III. Synthesis and characterization of a poly-yne polymer containing mixed metals in the main chain. *J. Organomet. Chem.* **1978**, *160*, 319–327. [[CrossRef](#)]
44. Lang, H.; Packheiser, R. Mixed transition metal acetylides connected by carbon-rich bridging units: On the way to heterohexametallic organometallics. *Collect. Czech. Chem. Commun.* **2007**, *72*, 435–452. [[CrossRef](#)]
45. Lavastre, O.; Even, M.; Dixneuf, P.H.; Pacreau, A.; Vairon, J.-P. Novel ruthenium-or iron-containing tetraynes as precursors of mixed-metal oligomers. *Organometallics* **1996**, *15*, 1530–1531. [[CrossRef](#)]
46. Zhou, G.J.; Wong, W.Y.; Lin, Z.; Ye, C. White Metallopolyyne for optical limiting/transparency trade-off optimization. *Angew. Chem. Int. Ed.* **2006**, *45*, 6189–6193. [[CrossRef](#)] [[PubMed](#)]
47. Zhou, G.J.; Wong, W.Y.; Ye, C.; Lin, Z. Optical power limiters based on colorless di-, oligo-, and polymetallaynes: Highly Transparent materials for eye protection devices. *Adv. Funct. Mater.* **2007**, *17*, 963–975. [[CrossRef](#)]
48. Vicente, J.; Chicote, M.-T.; Alvarez-Falcón, M.M.; Jones, P.G. Platinum (II) and mixed platinum (II)/gold (I) σ -alkynyl complexes. The first anionic σ -alkynyl metal polymers. *Organometallics* **2005**, *24*, 2764–2772. [[CrossRef](#)]
49. Zhou, G.; He, Y.; Yao, B.; Dang, J.; Wong, W.Y.; Xie, Z.; Zhao, X.; Wang, L. Electrophosphorescent Heterobimetallic oligometallaynes and their applications in solution-processed organic light-emitting devices. *Chem.-Asian J.* **2010**, *5*, 2405–2414. [[CrossRef](#)] [[PubMed](#)]
50. Chong, S.H.-F.; Lam, S.C.-F.; Yam, V.W.-W.; Zhu, N.; Cheung, K.-K.; Fathallah, S.; Costuas, K.; Halet, J.-F. Luminescent heterometallic branched alkynyl complexes of Rhenium (I)–Palladium (II): Potential building blocks for heterometallic metallodendrimers. *Organometallics* **2004**, *23*, 4924–4933. [[CrossRef](#)]
51. Koutsantonis, G.A.; Jenkins, G.I.; Schauer, P.A.; Szczepaniak, B.; Skelton, B.W.; Tan, C.; White, A.H. Coordinating tectons: Bipyridyl-terminated group 8 alkynyl complexes. *Organometallics* **2009**, *28*, 2195–2205. [[CrossRef](#)]
52. Di Piazza, E.; Boilleau, C.; Vacher, A.; Merahi, K.; Norel, L.; Costuas, K.; Roisnel, T.; Choua, S.; Turek, P.; Rigaut, S. Ruthenium carbon-rich group as a redox-switchable metal coupling unit in linear trinuclear complexes. *Inorg. Chem.* **2017**, *56*, 14540–14555. [[CrossRef](#)]
53. Soliman, A.M.; Fortin, D.; Harvey, P.D.; Zysman-Colman, E. Hybrid charged heterometallic Pt–Ir complexes: Tailoring excited states by taking the best of both worlds. *Chem. Commun.* **2012**, *48*, 1120–1122. [[CrossRef](#)] [[PubMed](#)]
54. Soliman, A.M.; Fortin, D.; Zysman-Colman, E.; Harvey, P.D. Unexpected evolution of optical properties in Ir–Pt complexes upon repeat unit increase: Towards an understanding of the photophysical behaviour of organometallic polymers. *Chem. Commun.* **2012**, *48*, 6271–6273. [[CrossRef](#)]
55. Soliman, A.M.; Fortin, D.; Zysman-Colman, E.; Harvey, P.D. Photonics of a conjugated organometallic Pt–Ir polymer and its model compounds exhibiting hybrid CT excited states. *Macromol. Rapid Commun.* **2012**, *33*, 522–527. [[CrossRef](#)] [[PubMed](#)]
56. Soliman, A.M.; Zysman-Colman, E.; Harvey, P.D. Strategic modulation of the photonic properties of conjugated organometallic Pt–Ir polymers exhibiting hybrid ct-excited states. *Macromol. Rapid Commun.* **2015**, *36*, 627–632. [[CrossRef](#)] [[PubMed](#)]

57. Khan, M.S.; Al-Mandhary, M.R.A.; Al-Suti, M.K.; Hisahm, A.K.; Raithby, P.R.; Ahrens, B.; Mahon, M.F.; Male, L.; Marseglia, E.A.; Tedesco, E.; et al. Structural characterisation of a series of acetylide-functionalised oligopyridines and the synthesis, characterisation and optical spectroscopy of platinum di-ynes and poly-ynes containing oligopyridyl linker groups in the backbone. *J. Chem. Soc. Dalton Trans.* **2002**, 1358–1368. [[CrossRef](#)]
58. Li, L.; Ho, C.-L.; Wong, W.-Y. Versatile control of the optical bandgap in heterobimetallic polymers through complexation of bithiazole-containing polyplatinynes with $\text{ReCl}(\text{CO})_5$. *J. Organomet. Chem.* **2012**, *703*, 43–50. [[CrossRef](#)]
59. Al-Khalili, A.N.; Al-Busaidi, I.J.; Ilmi, R.; Al-Mandhary, M.; Khan, M.S.; Al-Rasbi, N.K. Investigation of binding tendency of Eu(III) and La(III)-Schiff base complexes to selected oxy-anions and amino acids. *Inorg. Chim. Acta* **2020**, *501*, 119226. [[CrossRef](#)]
60. Binnemans, K. Interpretation of europium(III) spectra. *Coord. Chem. Rev.* **2015**, *295*, 1–45. [[CrossRef](#)]
61. Buenzli, J.C.G. *Lanthanide Probes in Life, Chemical and Earth Sciences*; Elsevier: Amsterdam, The Netherlands, 1989.
62. Ilmi, R.; Khan, M.S.; Li, Z.; Zhou, L.; Wong, W.-Y.; Marken, F.; Raithby, P.R. Utilization of Ternary Europium Complex for Organic Electroluminescent Devices and as a Sensitizer to Improve Electroluminescence of Red-Emitting Iridium Complex. *Inorg. Chem.* **2019**, *58*, 8316–8331. [[CrossRef](#)]
63. Li, J.; Wang, J.-Y.; Chen, Z.-N. Sensitized Eu(III) luminescence through energy transfer from PtM₂ (M=Ag or Au) alkynyl chromophores in PtM₂Eu₂ heteropentanuclear complexes. *J. Mater. Chem. C* **2013**, *1*, 3661–3668. [[CrossRef](#)]
64. Ward, M.D. Transition-metal sensitised near-infrared luminescence from lanthanides in d-f heteronuclear arrays. *Coord. Chem. Rev.* **2007**, *251*, 1663–1677. [[CrossRef](#)]
65. Lis, S.; Elbanowski, M.; Mąkowska, B.; Hnatejko, Z. Energy transfer in solution of lanthanide complexes. *J. Photochem. Photobiol. A Chem.* **2002**, *150*, 233–247. [[CrossRef](#)]
66. Etchells, I.M.; Pfrunder, M.C.; Williams, J.A.G.; Moore, E.G. Quantification of energy transfer in bimetallic Pt(II)-Ln(III) complexes featuring an N⁺C⁻N-cyclometalating ligand. *Dalton Trans.* **2019**, *48*, 2142–2149. [[CrossRef](#)]
67. Wong, W.Y.; Ho, C.L. Organometallic photovoltaics: A new and versatile approach for harvesting solar energy using conjugated polymetallaynes. *Acc. Chem. Res.* **2010**, *43*, 1246–1256. [[CrossRef](#)] [[PubMed](#)]
68. Jayapal, M.; Haque, A.; Al-Busaidi, I.J.; Al-Balushi, R.; Al-Suti, M.K.; Islam, S.M.; Khan, M.S. Synthesis, characterization and photocell studies of a Pt(II) poly-yne covalently attached to a fullerene. *J. Organomet. Chem.* **2017**, *842*, 32–38. [[CrossRef](#)]
69. Chawdhury, N.; Kohler, A.; Friend, R.H.; Wong, W.Y.; Lewis, J.; Younus, M.; Raithby, P.R.; Corcoran, T.C.; Al-Mandhary, M.R.A.; Khan, M.S. Evolution of lowest singlet and triplet excited states with number of thienyl rings in platinum poly-ynes. *J. Chem. Phys.* **1999**, *110*, 4963–4970. [[CrossRef](#)]
70. Ziessel, R.; Diring, S.; Kadjane, P.; Charbonnière, L.; Retaillieu, P.; Philouze, C. Highly Efficient Blue Photoexcitation of Europium in a Bimetallic Pt–Eu Complex. *Chem.-Asian J.* **2007**, *2*, 975–982. [[CrossRef](#)] [[PubMed](#)]
71. Xu, H.-B.; Zhang, L.-Y.; Xie, Z.-L.; Ma, E.; Chen, Z.-N. Heterododecanuclear Pt₆Ln₆ (Ln = Nd, Yb) arrays of 4-ethynyl-2,2'-bipyridine with sensitized near-IR lanthanide luminescence by Pt → Ln energy transfer. *Chem. Commun.* **2007**, 2744–2746. [[CrossRef](#)]
72. Xu, H.-B.; Zhang, L.-Y.; Chen, Z.-H.; Shi, L.-X.; Chen, Z.-N. Sensitization of lanthanide luminescence by two different Pt → Ln energy transfer pathways in PtLn₃ heterotetranuclear complexes with 5-ethynyl-2,2'-bipyridine. *Dalton Trans.* **2008**, 4664–4670. [[CrossRef](#)]
73. Xu, H.-B.; Ni, J.; Chen, K.-J.; Zhang, L.-Y.; Chen, Z.-N. Preparation, Characterization, and Photophysical Properties of cis- or trans-PtLn₂ (Ln = Nd, Eu, Yb) Arrays with 5-Ethynyl-2,2'-bipyridine. *Organometallics* **2008**, *27*, 5665–5671. [[CrossRef](#)]
74. Belyaev, A.; Slavova, S.O.; Solov'yev, I.V.; Sizov, V.V.; Jänis, J.; Grachova, E.V.; Koshevoy, I.O. Solvatochromic dual luminescence of Eu–Au dyads decorated with chromophore phosphines. *Inorg. Chem. Front.* **2020**, *7*, 140–149. [[CrossRef](#)]
75. Li, X.-L.; Dai, F.-R.; Zhang, L.-Y.; Zhu, Y.-M.; Peng, Q.; Chen, Z.-N. Sensitization of lanthanide luminescence in heterotrinnuclear PtLn₂ (Ln = Eu, Nd, Yb) complexes with terpyridyl-functionalized alkynyl by energy transfer from a platinum (II) alkynyl chromophore. *Organometallics* **2007**, *26*, 4483–4490. [[CrossRef](#)]
76. Jana, A.; Crowston, B.J.; Shewring, J.R.; McKenzie, L.K.; Bryant, H.E.; Botchway, S.W.; Ward, A.D.; Amoroso, A.J.; Baggaley, E.; Ward, M.D. Heteronuclear Ir (III)–Ln (III) luminescent complexes: Small-molecule probes for dual modal imaging and oxygen sensing. *Inorg. Chem.* **2016**, *55*, 5623–5633. [[CrossRef](#)] [[PubMed](#)]
77. Fernández-Moreira, V.; Marzo, I.; Gimeno, M.C. Luminescent Re (I) and Re (I)/Au (I) complexes as cooperative partners in cell imaging and cancer therapy. *Chem. Sci.* **2014**, *5*, 4434–4446. [[CrossRef](#)]
78. Zhao, H.; Simpson, P.V.; Barlow, A.; Moxey, G.J.; Morshedi, M.; Roy, N.; Philip, R.; Zhang, C.; Cifuentes, M.P.; Humphrey, M.G. Syntheses, spectroscopic, electrochemical, and third-order nonlinear optical studies of a hybrid tris {ruthenium (alkynyl)/(2-phenylpyridine)} iridium complex. *Chem. Eur. J.* **2015**, *21*, 11843–11854. [[CrossRef](#)]
79. Haque, A.; Faizi, M.S.H.; Rather, J.A.; Khan, M.S. Next generation NIR fluorophores for tumor imaging and fluorescence-guided surgery: A review. *Biorg. Med. Chem.* **2017**, *25*, 2017–2034. [[CrossRef](#)] [[PubMed](#)]
80. Zhu, Q.-Y.; Zhou, L.-P.; Sun, Q.-F. Strongly luminescent 5d/4f heterometal–organic macrocycles with open metal sites: Post-assembly modification and sensing. *Dalton Trans.* **2019**, *48*, 4479–4483. [[CrossRef](#)] [[PubMed](#)]
81. Zhu, Q.-Y.; Zhou, L.-P.; Cai, L.-X.; Li, X.-Z.; Zhou, J.; Sun, Q.-F. Chiral auxiliary and induced chiroptical sensing with 5d/4f lanthanide–organic macrocycles. *Chem. Commun.* **2020**, *56*, 2861–2864. [[CrossRef](#)]